

Modified models to predict the ultimate flexural and shear capacities of CFRP repaired RC beams

Moatasem M. Fayyadh^{*1,2}

¹Engineering Services & Asset Management, John Holland Group, 2150 NSW, Australia

²Department of Civil Engineering, University of Malaya, 50603 Kuala Lumpur, Malaysia

(Received August 5, 2020, Revised December 2, 2020, Accepted January 22, 2021)

Abstract. Research is still ongoing to establish accurate models to predict the ultimate capacity of carbon fiber reinforced polymer (CFRP) repaired Reinforced Concrete (RC) beams, despite the numerous studies that have been conducted in this area. Previous studies suggested that more research is needed to better understand concrete behavior at flexural and shear, as well as the interaction between RC beams and externally bonded CFRP sheets. This study aims to experimentally validate the equations provided by the ACI 440.2 code for calculating the ultimate flexural and shear capacity of damaged RC beams repaired with CFRP sheets. The two design criteria for flexural capacity are the minimum and maximum steel ratios. Likewise, the two design criteria for shear capacity are having and not having shear stirrups. Moreover, two shear locations are investigated as the shear capacity at the quarter-span and shear capacity at 1.5d (d is the beam depth from supports). Finally, modified models are proposed to calculate the flexural and shear capacities, considering the contributions from other parameters to better correlate with the experimental results. The study concluded that the current ACI models result in differences from experimental results of up to 21%, 64% and 25% for flexural capacity, shear capacity at quarter-span and shear capacity at 1.5d, respectively. The modified models result in differences from experimental models of 6.9%, 2% and 7.3% for flexural capacity, shear capacity at quarter-span and shear capacity at 1.5d, respectively.

Keywords: CFRP repair; flexural capacity; shear capacity; contribution factors; concrete reduction factor; RC structures; design criteria; damage location

1. Introduction

Research on the use of carbon fibre reinforced polymer (FRP) began in Europe in the 1960s (Bakis *et al.* 2002). The first investigation into the use of FRP plate bonding took place at the Swiss Federal Laboratory for Materials Testing and Research (EMPA) in 1984 (Teng *et al.* 2001). FRP materials have the advantages of high tensile strength and excellent corrosion resistance, fatigue resistance, good performance at elevated temperatures, low density and high specific stiffness and strength (Meier 1992).

Most research on using FRP plate bonding for flexural strengthening was carried out over the last few decades (Saadatmanesh *et al.* 1991, Triantafillou and Plevris 1992). There has been

*Corresponding author, Ph.D., E-mail: Moatasem.m.f@gmail.com

tremendous growth in recent years because of the increasing global need for an improved structural performance to improve and retrofit works. Repairing a real bridge with externally bonded FRP plates was found to decrease the flexural stresses in the steel reinforcements and the mid-span deflection (Stallings *et al.* 2000). Strengthening the RC beam with one layer of the CFRP plate was found to increase the ultimate capacity by 200%, and strengthening with two layers increased it by 250% (Capozucca and Cerri 2002). Fayyadh and Razak (2012) used the flexural stiffness change in the index to evaluate the effectiveness of CFRP repaired RC beams and found that the CFRP repair system recovered stiffness and increased the load capacity by up to 83%. CFRP plates increase the ultimate load and decrease the mid-span deflection and pre repair damage level, which has a significant impact on the repair effectiveness (Fayyadh and Razak 2014). Al-Khafaji and Salim (2020) investigated strengthening RC continuous T-beams with CFRP sheets and found that the strengthened beams' ultimate capacity increased by up to 90%. Additionally, regarding the strengthened beams with a CFRP-to-beam width ratio of below 0.25, the strengthening system did not increase stiffness. However, they still increased in ductility. Vuković *et al.* (2020) conducted an experimental analysis of RC elements strengthened with CFRP strips to determine the contribution of a composite material to improve the mechanical behaviour of old, full size RC T-beams in operating condition. They found that to strengthen the supported beams, there was no need to extend the CFRP strip longer than half the span length, and lateral anchorages were not required.

Studies on the use of FRP plate bonding for shear strengthening began in the 1990s (Al-Sulaimani *et al.* 1994, Malek and Saadatmanesh 1998, Khalifa and Nanni 2000). However, they are still limited compared to the studies on the use of FRP plates for flexural strengthening (Teng *et al.* 2001). The strengthened beam stiffness was found to increase with the increase in the CFRP plates' area on the beams' sides, which also delayed the appearance of the first flexural cracks (Li *et al.* 2001). The use of u-shape anchored CFRP sheets for shear strengthening can increase the capacity by up to 20% (El-Ghandour 2011). Ahmed *et al.* (2015) investigated the effect of plate thickness on the shear repair effectiveness of CFRP and steel-plated RC beams with a web opening and found that an increase in the steel plate thickness had an insignificant effect on the maximum load capacity, whereas the CFRP plate thickness had a more significant effect on the ultimate load capacity. Ahmed *et al.* (2016) investigated the shear repair effectiveness of CFRP and steel-plated RC beams with a web opening and found that both CFRP and steel plates were an effective repair solution. However, the CFRP plates performed better, and the rectangular configurator was better than the hexagonal one.

Many studies that were carried out over the last decade dealt with the equations and principles used to calculate the FRP bonded plate contribution to the capacity of the strengthening/repaired beams. Most research suggests using the same design procedure for the unstrengthened beams while taking into consideration the brittle nature of the FRP plates (Malek and Saadatmanesh 1998). Therefore, many design equations and guidelines were proposed for calculating the flexural capacity of the strengthened RC beams with bonded FRP plates based on the design approach of the ACI-318 code (Malek and Saadatmanesh 1998, El-Mihilmy *et al.* 2000, Lam and Teng 2001). The effect of the pre-strengthening or existing strain in the beam soffit on the FRP bonded plates' contribution to the flexural capacity was studied by Lam and Teng (2001), and the effect was considered in the design equations, as shown by Saadatmanesh *et al.* (1998). During the last decade, many studies proposed mathematical models to calculate the FRP plate's contribution to the shear capacity of the strengthened beams (Chaallal *et al.* 1998, Khalifa *et al.* 1998, Chen and Teng 2001, Chen and Teng 2003). A simple approach for the design of the concrete beams

strengthened with an externally bonded FRP plate was proposed, where the maximum and minimum limits of the FRP plate were established (El-Mihilmy and Tedesco 2000). A truss model was proposed for predicting the ultimate shear capacity and behaviour of strengthened beams with externally bonded FRP plates (Colotti and Spadea 2001). A straightforward approach for the design of the concrete beam strengthened with externally bonded FRP plates was proposed by Malek *et al.* (2002). The contribution of the FRP plate to the ultimate shear capacity of the strengthened beams depends on the quantity of the FRP and the ratio between the steel stirrup and the FRP plates (Pellegrino and Modena 2002). The shear capacity of the strengthened beam with an externally bonded FRP plate was calculated using the ACI-440R 1996 guidelines and was 20% less than the experimental results (Anil 2006). A partial interaction model for the quantification of the interaction between the shear steel stirrups and the external bonded FRP plates and its contribution to the ultimate shear capacity was developed, and it was found to be a complex problem since although the steel stirrups yielded, the FRP ruptured. It was concluded that more research needs to be done for a better understanding of the interaction between the internal stirrups and external FRP plates (Mohamed-Ali *et al.* 2006). Using the equations of ACI-440-2R 2002 for predicting the CFRP plate contribution to the ultimate shear capacity resulted in larger values than the experiential results (Dias and Barros 2010). Using the equations of ACI-440-2R 2002 for the calculation of the CFRP sheet contribution to the capacity of the strengthened deep RC beams showed an overestimate compared to the experimental results (Lee *et al.* 2011). Shaw and Andrawes (2017) studied the effect of accelerated aging on CFRP laminate repair effectiveness and found that the repair system was effective, regardless the environmental aging condition. Al-Karkhi and Aziz (2018) investigated the effect of CFRP strips on the shear strength of the self-compacting concrete hammer head beams and concluded that the strengthened beams enhanced the shear capacity by up to 30%. El-Taly *et al.* (2018) investigated the performance enhancement of precast-prestress hollow core slabs strengthened with GFRP and CFRP strips and near surface mounted GFRP bars and found that the GFRP strips were the most effective repair system. Additionally, they found that adopted strengthening systems enhance ductility and energy observation. Xie and Wang (2019) conducted a reliability analysis of the CFRP repaired RC bridges, and considering the effect of the CFRP sizes, concluded that the CFRP strengthening system effectively improved the safety of structures, irrespective of the CFRP size. Strengthening the RC column with CFRP, subject to eccentric loading, showed a significant improvement to the ultimate capacity and ductility (Alhawamdeh and Alqam 2020).

The American Concrete Institute (ACI) started to consider the FRP bonded plate as construction material, and their first work on the FRP plate was a state-of-the-art report on the use of the FRP for concrete structures in 1996 (ACI-440R 1996). The first design guidelines for the use of fibre composite materials were released by the ACI-440-2R (2000), followed by guidelines for the design of an externally bonded FRP system in ACI-440-2R (2002). The work in the ACI was continually updated regarding the use of the externally bonded FRP plate or using FRP bars as reinforcement, according to the findings of new research and the arising needs (ACI-440.3R 2004, ACI-440R 2007, ACI-440.2R 2008).

Although many studies have been carried out regarding the flexural and shear designs of RC structures repaired with an externally bonded CFRP sheet, research is still ongoing for failure mechanisms and predicting the ultimate capacity. Based on previous studies, more research needs to be done for a better understanding of concrete behaviour at the flexural and shear capacities and interaction with CFRP sheets. Therefore, this study aims to evaluate the equations provided by the ACI 420.2 code to predict the flexural and shear ultimate load capacities of RC beams repaired

Table 1 Classification according to damage scenario, design case and damage level

| Beam No. | Damage Location | Design Case | Pre-repair damage level |
|----------|-----------------------|------------------|-------------------------------|
| B122 m | Flexural | ρ_{min} | Design load limit |
| B123 m | Flexural | ρ_{min} | Steel yield load limit |
| B124 m | Flexural | ρ_{min} | Failure load |
| B112 m | Flexural | ρ_{max} | Design load limit |
| B113 m | Flexural | ρ_{max} | Steel yield load limit |
| B114 m | Flexural | ρ_{max} | Failure load |
| B212 q | Shear at quarter-span | With stirrups | Design load limit |
| B211 q | Shear at quarter-span | With stirrups | Failure load |
| B222 q | Shear at quarter-span | Without stirrups | Design load limit |
| B221 q | Shear at quarter-span | Without stirrups | Failure load |
| B211 d | Shear at 1.5 d | With stirrups | Failure load |
| B212 d | Shear at 1.5 d | With stirrups | Maximum load prior to failure |
| B221 d | Shear at 1.5 d | Without stirrups | Failure load |
| B222 d | Shear at 1.5 d | Without stirrups | Maximum load prior to failure |

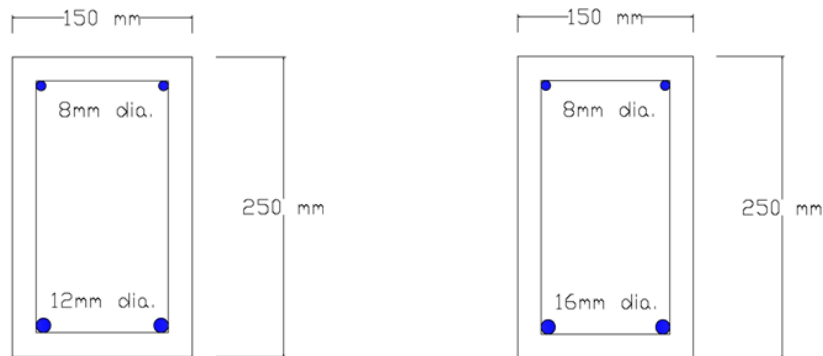


Fig. 1 Cross section detail for flexural beams, with ρ_{min} (left) and with ρ_{max} (right)

with CFRP sheets.

2. Experimental work program

A total of 14 reinforced concrete beams were prepared for this study. These were divided into the following three damage location scenarios: flexural damage at mid-span with total of six beams; shear damage at quarter-span with total of four beams; and shear damage at 1.5 d (d is the effective beam depth) with a total of four beams.

Two design criteria for the flexural case were adopted as the minimum (ρ_{min}) and maximum (ρ_{max}) flexural steel limit. Two design criteria for the shear cases were adopted as RC beams with shear steel stirrups and RC beams without shear steel stirrups.

Modified models to predict the ultimate flexural and shear capacities of CFRP repaired RC beams

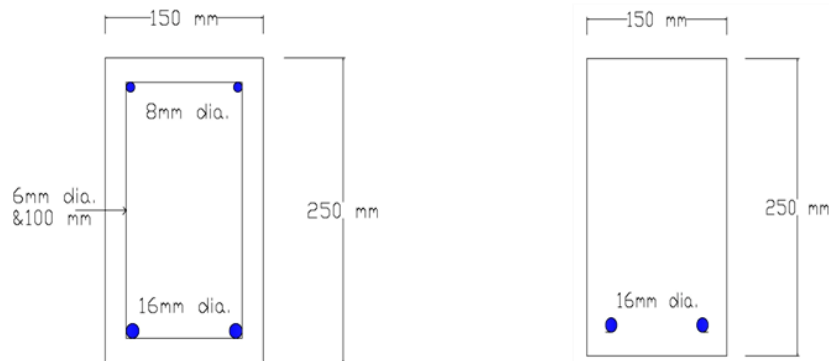


Fig. 2 Cross section detail for shear beams, with stirrups (left) and without stirrups (right)

Table 2 Concrete and Steel material properties

| Beam No. | Concrete Compressive strength (MPa) | Concrete Elasticity Modulus (GPa) | Steel Yield Stress (MPa) | Steel Rapture Stress (MPa) | Steel Elasticity Modulus (GPa) |
|----------|-------------------------------------|-----------------------------------|--------------------------|----------------------------|--------------------------------|
| B122 m | 36 | 30 | 535 | 665 | 180 |
| B123 m | 36 | 33 | 565 | 785 | 180 |
| B124 m | 35 | 31 | 565 | 785 | 180 |
| B112 m | 38 | 36 | 480 | 620 | 180 |
| B113 m | 33 | 29 | 520 | 680 | 180 |
| B114 m | 30 | 34 | 480 | 620 | 180 |
| B212 q | 33 | 30 | 520 | 680 | 180 |
| B211 q | 32.3 | 29 | 520 | 680 | 180 |
| B222 q | 41 | 36 | 520 | 680 | 180 |
| B221 q | 38 | 35 | 520 | 680 | 180 |
| B211 d | 36 | 33 | 520 | 680 | 180 |
| B212 d | 33 | 30 | 520 | 680 | 180 |
| B221 d | 42 | 37 | 520 | 680 | 180 |
| B222 d | 40 | 36 | 520 | 680 | 180 |

Three pre-repair damage levels were considered for the flexural scenario, which were the damage at design load limit, damage at steel yield load limit and damage at failure load. Two pre-repair damage scenarios were considered for the shear damage at quarter span, which were the damage at design load limit and damage at failure load. Additionally, two pre-repair damage levels were considered for the shear damage at 1.5 d, which were the damage at maximum load prior to failure and damage at fully failure load. Table 1 presents the classification of the tested RC beams.

The clear span length for each beam was 2.2 m, with a beam cross section of 150 mm and a width of 250 mm. For the flexural structural design of the pre-repaired beams, ACI 318 (2008) was used. Based on the ACI Code, there was provision for two limits of the steel ratio in the tension layer, as the reinforcement requirements for the structural elements are subjected to flexure. The p_{min} was provided to prevent cracking due to thermal expansion, and the p_{max} was provided to prevent brittle failure due to the crushing of concrete. Therefore, this study takes into consideration

the two steel ratio limits. The flexural beams were designed in shear capacity to ensure that the beam would not fail in shear failure by using shear stirrups with close spacing to ensure a high shear resistance. The procedure of the design for the flexural capacity using both ρ_{min} , ρ_{max} and the shear design to achieve the highest shear resistance was in accordance with the ACI 318 (2008) equations. For the ρ_{max} , two 16 mm diameter deformed steel bars were used as the main flexural reinforcement, whereas for the ρ_{min} , two 12 mm diameter deformed steel bars were used as the main flexural reinforcement. For both design cases, two 8 mm diameter round steel bars were used as the compression reinforcement, and for the shear design, 6 mm diameter bars with a spacing of 50 mm were used along the beam length to achieve the highest shear resistance. Fig. 1 shows the cross-section detail for the flexural beams, i.e., ρ_{min} and ρ_{max} .

For the shear structural design of the pre-repaired beams, ACI 318 (2008) was used. The following two shear design cases were used: one with internal shear stirrups in which the shear forces were resisted by the stirrups and concrete; and another without the internal shear stirrups in which all the shear forces were resisted solely by the concrete. This study will consider both design cases, with and without shear stirrups.

The RC beams were designed to resist a concentrated load located at the quarter-span or at 1.5d from the support, in addition to the self-weight of the beams. The shear group beams were designed in flexural capacity to ensure that the beam would not fail in flexural capacity by using flexural steel bars with ρ_{max} to ensure a high flexural capacity. The procedure of the shear design for both cases, with and without shear stirrups, as well as the flexural design to achieve the highest flexural capacity, was in accordance with the ACI 318 (2008) equations. For the group without shear stirrups, two 16 mm diameter deformed steel bars were used as the main flexural reinforcement, and no shear stirrups were used. For the group with stirrups, 6 mm diameter steel bars with spacing of 100 mm c/c were used as shear stirrups, two 16 mm diameter deformed steel bars were used as the main flexural reinforcement and two 8 mm diameter non-deformed steel bars were used as the compression reinforcement. The same design was adopted for both shear damage scenarios at quarter-span and 1.5d from the supports. Fig. 2 shows the cross-section detail at the shear zone of the RC beams of both cases, with and without shear stirrups.

The concrete material properties in terms of compressive strength and modulus of elasticity and the steel reinforcement material properties in term of yield stress, rupture stress and modulus of elasticity of the 14 tested beams are shown in Table 2.

The ACI 420.2R (2002) was used as the design guidelines for externally bonded CFRP for repairing the RC structures. The design of the flexural repair with externally bonded CFRP sheets was based on achieving the maximum capacity without debonding failure of the CFRP sheets to achieve the highest CFRP strength. The design procedure was in accordance with the ACI 420.2R (2002) equations. For the ρ_{min} group, a CFRP sheet with 100 mm width and 1.2 mm thickness gave the highest increase in the capacity before the CFRP debonding. For the ρ_{max} group, a CFRP sheet with 50 mm width and 1.2 mm thickness gave the highest increase in the capacity before CFRP debonding. The CFRP sheets were designed to be placed on the beam soffit and along the beam length between the supports.

The ACI 420.2R (2002) was used as the design guidelines for repairing damaged beams in shear with externally bonded CFRP sheets. The objective of the repair with CFRP sheets design was to achieve the highest capacity using the CFRP sheets within the limits of the ACI Codes. For the shear at quarter-span, three CFRP sheets with a width of 100 mm and thickness of 1.2 mm were used on both sides of the beam between the quarter-span and the support within an inclined angle of 45°. For the shear damage at 1.5d from the support, two configurations were used. The

Modified models to predict the ultimate flexural and shear capacities of CFRP repaired RC beams



Fig. 3 Surface preparation and CFRP fixing for flexural and shear

Table 3 CFRP material properties

| | Longitudinal direction |
|-----------------------------|------------------------|
| Tensile strength (MPa) | 2,800 |
| Modulus of Elasticity (MPa) | 165,000 |
| Ultimate strain (mm/mm) | 0.017 |

first configuration consisted of two CFRP sheets of 100 mm width and 1.2 mm thickness with an inclined angle of 45° . The second configuration used two CFRP sheets of 100 mm width and 50 mm width, respectively, placed vertically to cover the distance between the $1.5d$ and the support.

Sika-Carbo-Dur S1012 sheets were used as shear repair systems. The properties of the CFRP sheets were the same as the SIKA data sheet (refer to Table 3). Since the CFRP sheets that were used were externally bonded, the Sikadur-30, which is the product of SIKA, was used as the adhesive layer between the CFRP sheets and the concrete surface. The tension face was roughened to create a suitable face to give as much friction as possible with the CFRP sheet. Fig. 3 shows the roughened surface that was prepared by using a scaling hammer and fixing the CFRP sheets. The surface was cleaned using an air gun to remove any dust on the surface, as the substrates must be sound, dry, clean and free from laitance, standing water, grease, oils, old surface treatments or coatings and all loosely adhering particles. The concrete was cleaned and prepared to achieve a laitance and contaminant-free, open-textured surface. When the concrete surface was prepared, the CFRP sheet was fixed using Sikadur-30 adhesive material, and it was then left for to harden for one month to avoid the effect of the adhesive setting time on the dynamic properties, as advised by Fayyadh and Razak (2013).

A static test was used in this study to induce damage to the RC beams at the pre-repair damage stage, as per the damage levels illustrated in Table 1 above. Following that, the load at the post-repair stage was applied to find the ultimate failure load. The static load test included the application of a concentrated load to the RC beams at different locations to induce damage, as

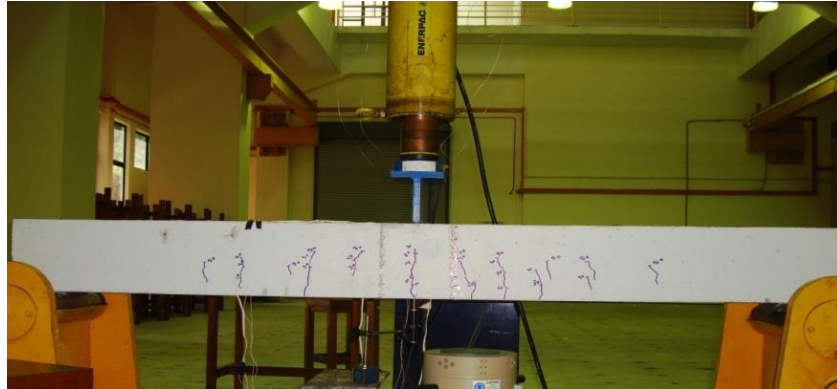


Fig. 4 Beam under static test – flexural scenario

Table 4 Results for the repaired flexural beams - original ACI model

| Beam | Case | Ultimate load capacity (kN) | | | CFRP debonding strain (μst) | | |
|--------|--|-----------------------------|----------|--------|--|----------|--------|
| | | Experimental | ACI Code | Dif. % | Experimental | ACI Code | Dif. % |
| B122 m | ρ_{\min} & Damage at design load limit | 131 | 103.4 | -21.0 | 6100 | 6780 | 11.1 |
| B123 m | ρ_{\min} & Damage at steel yield load limit | 130.7 | 105.2 | -19.5 | 5400 | 5900 | 9. |
| B124 m | ρ_{\min} & Damage at Failure load | 128 | 101 | -21.1 | 5890 | 5460 | -7.3 |
| B112 m | ρ_{\max} & Damage at design load limit | 120 | 104.2 | -13.1 | 5550 | 5980 | 7.7 |
| B113 m | ρ_{\max} & Damage at steel yield load limit | 124.7 | 105.4 | -15.5 | 5400 | 5150 | -4.6 |
| B114 m | ρ_{\max} & Damage at Failure load | 94.5 | 90 | -4.8 | 4790 | 4400 | -8.1 |

illustrated in Table 1 above, i.e., the load at mid-span for the flexural scenario, the load at quarter-span for the shear scenario and the load at $1.5d$ for the shear scenario at $1.5d$ from the support. A steel frame was used to apply the load using a load actuator controlled by a servo hydraulic pump. The load was applied gradually at a loading rate of 0.75 kN/min in cycles of loading and unloading. A 50 mm displacement transducer was placed at the point of the maximum deflection to measure the displacement. The load cell of the 250 kN capacity was placed directly below the hydraulic load actuator to measure the loads, as shown in Fig. 4. The CFRP sheets strain was measured using strain gauges fixed on the CFRP sheets' surface at the maximum expected strain positions.

3. Results and discussion

After carrying out the static tests and obtaining the ultimate loads for the CFRP repaired RC beams with flexural and shear capacities, the ACI model's results for predicting the ultimate capacities were compared to the experimental work. For the purpose of the evaluation, and since the comparison with the experimental results was based on the ultimate capacity, all the safety

factors were neglected from the ACI equations to find the actual ultimate capacity of the RC beams.

3.1 Repaired RC beams in flexural

This section presents the comparison between the ACI model and experimental results for the flexural repaired RC beams. The comparison covers both flexural reinforcement ratios, which are the ρ_{min} (B122 m, B123 m and B124 m) and ρ_{max} (B112 m, B113 m and B114 m) groups. The comparison highlights the values of the ultimate load capacity and CFRP debonding strain, as shown in Table 4. The CFRP debonding strain had a stronger agreement than the ultimate capacity results. For the ρ_{min} group beams, the ACI model results showed higher CFRP debonding strain values compared to the experimental results with a maximum difference of 11%, whereas for the ρ_{max} group beams, the ACI model results were smaller than the experimental results by a maximum difference of 8%. The difference in the CFRP debonding strain could be due to the assumption of the ACI model, which is the stress distribution corresponding to the depth of the cross section.

For the ultimate load capacity, the ACI model results show smaller values than the experimental results by 21.1% for the ρ_{min} group beams and around 15.5% for the ρ_{max} group. The differences between the ACI model and experimental results could be due to the ACI model's assumptions for the ultimate concrete crushing strain of 3000 $\mu\epsilon$, while the actual value can be higher. The ACI model advises not considering the steel reinforcement at the compression zone when calculating the ultimate capacity for the repaired section, which could be another reason for the smaller ACI model's results compared to the experimental results. In the actual repaired RC beam, the steel reinforcement at the compression zone was still working and sharing the compression stress. Therefore, the compression zone steel reinforcement can reduce the difference between the ACI model and the experimental results. The ultimate moment capacity of the repaired section according to the ACI Code is shown in Eq. (1) as follows:

$$Mu = A_{s1} \cdot f_{s1} \left(d - B1 \cdot \frac{c}{2} \right) + A_f \cdot f_f \left(h - B1 \cdot \frac{c}{2} \right) \quad (1)$$

Where Mu is the ultimate moment capacity, A_{s1} is the cross-section area of the main steel bars, f_{s1} is the ultimate stress of the main steel bars, d is the effective depth, c is the depth of the neutral axis, A_f is the CFRP cross section area, f_f is the CFRP ultimate stress and h is the beam depth

$$B1 = 0.85 - 0.008 (f_c - 30) \quad (2)$$

Where f_c is the concrete compressive strength.

To include the contribution of the steel bars at the compression zone, Eq. (1) can be re-written in the following form:

$$Mu = (A_{s1} - A_{s2}) \cdot f_{s1} \left(d - B1 \cdot \frac{c}{2} \right) + A_f \cdot f_f \left(h - B1 \cdot \frac{c}{2} \right) + A_{s2} \cdot f_{s2} (d - d') \quad (3)$$

Where A_{s2} is the cross-section area of the compression steel bars, f_{s2} is the ultimate stress of the compression steel bars and d' is the effective depth of the compression steel bars.

The ultimate load capacity based on the modified Eq. (3) of the ACI Code provides the results shown in Table 5. The modified ACI model provides closer results to the experimental data, where the difference decreases to less than 7% for all the beams. The modified ACI model's results remain smaller than the experimental results for all the beams except for beam B114 m, which

Table 5 Results for the repaired flexural beams - modified ACI model

| Beam | Ultimate load capacity (kN) | | |
|--------|-----------------------------|----------------|--------|
| | Experimental | Modified Model | Dif. % |
| B122 m | 131 | 122 | -6.9 |
| B123 m | 130.7 | 126 | -3.6 |
| B124 m | 128 | 120 | -6.3 |
| B112 m | 120 | 118.5 | -1.3 |
| B113 m | 124.7 | 116.7 | -6.4 |
| B114 m | 94.5 | 96 | 1.6 |

Table 6 Comparison of ACI Code and experimental results for repaired shear beam at quarter-span

| Beam | Case | Ultimate load capacity (kN) | | | CFRP debonding strain (μst) | | |
|-------|---|-----------------------------|----------|--------|--|----------|--------|
| | | Experimental | ACI Code | Dif. % | Experimental | ACI Code | Dif. % |
| B212q | With stirrups & Damaged at design load limit | 120 | 178.5 | 48.8 | 660 | 1490 | 125.8 |
| B211q | With stirrups & Damaged at ultimate load | 107 | 176.4 | 64.9 | 695 | 1460 | 110.1 |
| B222q | Without stirrups & Damaged at design load limit | 120 | 165.2 | 37.7 | 800 | 1750 | 118.8 |
| B221q | Without stirrups & Damaged at ultimate load | 101 | 155.3 | 53.8 | 720 | 1630 | 126.4 |

shows higher values than the experimental results by 1.6%.

3.2 Repaired RC beams in shear – damage at the quarter span

This section presents the comparison between the ACI Code and experimental results for the shear scenario when the load is applied at the quarter-span. The results for the repaired beams with CFRP sheets are presented. For the repaired shear beam, when the load is applied at the quarter-span, four beams are tested in two groups. The first group is designed with the shear stirrups, which is B211q and B212q, where beam B211q is damaged under the ultimate load capacity at the pre-repair damage stage, and beam B212q is damaged under the design load limit at the pre-repair damage stage. The second group is designed without the shear stirrups, which is B221q and B222q, where beam B221q is damaged under the ultimate load at the pre-repair damage stage, and B222q is damaged under the design load limit at the pre-repair damage stage. Based on the ACI model, to calculate the ultimate capacity for the repaired beam (V_R), the contribution of the concrete and the shear stirrups is shown in Eqs. (4) and (5).

$$V_c = 0.17 \sqrt{f_c} b d \quad (4)$$

$$V_s = A_v \cdot f_v \cdot d/s \quad (5)$$

Where f_c is the concrete compressive strength, b is the beam width, d is the effective depth, A_v is the cross-section area of the stirrups bar, f_v is the yield stress of the vertical stirrups and s is the

distance between the stirrups.

The extra contribution from the fixed externally bonded CFRP sheets V_f is described in Eq. (6) below;

$$V_f = \frac{A_f f_f (\sin \alpha + \cos \alpha) \cdot d_f}{S_f} \quad (6)$$

Where A_f is the cross section of the CFRP sheet on both sides, f_f is the tensile stress of the CFRP sheet, α is the angle at which the CFRP sheet is placed to the side of the beam, d_f is the effective depth of the CFRP sheet on the beam side and S_f is the spacing between the CFRP sheets.

The ultimate repair capacity in shear capacity as per the ACI model is shown in the following Eq. (7):

$$V_R = V_c + V_s + V_f \quad (7)$$

The comparison between the ACI Code model and the experimental results is based on the ultimate repair capacity and the maximum CFRP sheet strain at failure, and the results are shown in Table 6. The results showed significant differences between the ACI model and experimental results in terms of the ultimate shear capacity and CFRP strain at failure. The difference in the CFRP strain was higher than the ultimate shear capacity. For both the ultimate capacity and the CFRP strain values, the ACI model's results showed much higher values than the experimental results, which is an overestimate of the shear capacity. The repaired beams that were damaged under the ultimate load at the pre-repair damage stage showed a higher difference in terms of the ultimate capacity, and the beams without stirrups showed a lower difference than the beams with stirrups. The significant difference between the ACI model and the experimental results could be due to the assumptions of the ACI Code while calculating the contribution of the concrete, steel reinforcements and CFRP to the ultimate capacity.

The main considerations which can be taken into account when modifying the ACI Code equations are as follows:

- The ACI equations show no consideration for the pre-repair damage level in the calculation of the ultimate capacity in the repair stage.
- The contribution of the shear stirrups to the ultimate capacity is higher than the actual values, where beams with stirrups show a higher difference.
- The CFRP contribution to the ultimate capacity is higher than the actual values, where the CFRP strain is much higher than the actual values.

When the RC beam is subjected to a point load applied at a distance from the support, the concrete contribution to the ultimate capacity is the resisting force by the inclined area of the beam cross section, which is drawn with an angle of 45^0 (on average) from the support. The shear stirrups' contribution to the ultimate capacity is equal to the component of the shear stirrups and perpendicular to the inclined concrete surface. The modified contribution of both the concrete and shear stirrups to the ultimate shear capacity of the RC beams are shown in Eqs. (8) and (9) below (as modifications to Eqs. (4) and (5):

$$V'_c = 0.24 bh \sqrt{f_c} \quad (8)$$

$$V'_s = A_v \cdot f_v \cdot d \cdot \sin(45^0) / s \quad (9)$$

where V'_c and V'_s are the modified concrete and shear stirrups contribution to the ultimate shear

capacity and h is the beam depth.

According to the modified equation, the concrete contribution increases after considering the inclined effective depth, while the steel stirrups' contribution decreases after considering only the perpendicular component of the shear stirrups.

A reduction factor (RF_c) is proposed to be applied to the concrete contribution, which is based on the pre-repair damage level and will have a value of $0 \leq RF_c \leq 1.0$, with 0.0 for fully damaged beams at the pre-repair stage and 1.0 for undamaged beams. When the damage is induced in the shear zone, the contribution of the concrete is reduced based on the loss in the aggregate interlock at the shear crack zone.

A contribution factor (CF_f) for the CFRP sheets to the ultimate repaired shear capacity is proposed and applied to the V_f part of Eq. (7) to adjust the CFRP contribution based on the experimental results.

The flexural steel reinforcement, which crosses the inclined concrete surface, contributes to the ultimate shear capacity. To find the contribution of the flexural steel reinforcement to the ultimate shear capacity, first the stress in the flexural steel reinforcement must be established. The flexural steel stress can be calculated based on the moment of the beams at the section of the applied load. The total shear capacity of the beam at the section of the applied load is based on Eqs. 8 and 9 above.

For a concentrated load located at the quarter-span ($L/4$), the moment at the applied load section is as follows;

$$M = \frac{V * L}{4} \quad (10)$$

Where L is the clear span length and $V = V_c' + V_s'$.

The stress at the flexural steel bars (f_s) can be calculated using the trial-and-error procedure based on the following equations:

$$a = \frac{A_s \cdot f_s}{0.85 \cdot f_c \cdot b} \quad (11)$$

$$M = A_s \cdot f_s \cdot (d - a/2) \quad (12)$$

Where A_s is the cross section area of the flexure bars and a is the depth of the concrete compressive steel.

After calculating the flexural steel stress (f_s), the force V_m can be calculated as follows:

$$V_m = A_s \cdot F_s \quad (13)$$

The contribution of the flexural steel to the ultimate shear capacity of the RC beam is calculated based on the perpendicular component of force V_m to the inclined concrete surface. A contribution factor (CF_m) is used to indicate the amount of shared force that can be taken by the main flexural steel bars. The flexural contribution can be calculated as follows:

$$V_M' = CF_m \cdot A_s \cdot f_s \cdot \sin (45^\circ) \quad (14)$$

where V_M' is the flexural steel contribution to the ultimate shear capacity and CF_m is the contribution factor of the main steel with a value of $0 \leq CF_m \leq 1.0$, which depends on the location of the applied load and the presence of the shear stirrups.

The contribution of the flexural steel to the shear capacity is considered, and the same

Table 7 Comparison of modified ACI model and experimental results for repair shear beam at quarter-span

| Beam | Case | Ultimate load capacity (kN) | | |
|-------|---|-----------------------------|------------------------|--------|
| | | Experimental | Modified ACI equations | Dif. % |
| B212q | With stirrups & Damaged at design load limit | 120 | 116.4 | -3 |
| B211q | With stirrups & Damaged at ultimate load | 107 | 105 | -1.9 |
| B222q | Without stirrups & Damaged at design load limit | 120 | 119.3 | -0.6 |
| B221q | Without stirrups & Damaged at ultimate load | 101 | 100.8 | -0.2 |

procedure as Eqs. (8) to (14) is used. CF_m of 0.1 is used for the beams without stirrups, and CF_m of 0.01 is used for beams with stirrups.

The modified equation of the CFRP repaired beams' shear capacity can be written as follows:

$$V_R' = CF_f \cdot V_f + RF_c \cdot V_c' + V_s' + CF_m \cdot V_m' \quad (15)$$

The comparison results based on the modified ACI Code equations are shown in Table 7. The modified ACI model's equation results are in better agreement with the experimental results in terms of the ultimate capacity, where the maximum difference is less than 3%. All the calculated ultimate capacity values from the modified ACI Code equation are smaller than the experimental results. The reduction factor for the concrete contribution (RF_c) is equal to 0.15 for beams B212q and B222q, which were subjected to the design limit load at the pre-repair damage stage, and 0.0 for beams B211q and B221q, which were subjected to the maximum load at the pre-repair damage stage where the concrete lost all of its stiffness. The CFRP contribution factor (CF_f) is equal to 0.78 for all the pre-repair damage levels and for both design cases, which is with and without the steel stirrups.

3.3 Repaired RC beams in shear – damage at 1.5d

For the repaired shear beam, when the load was applied at 1.5d from the supports, four beams were used and repaired after damage at the maximum load capacity. Beams B212d and B222d were subjected to the maximum load at the pre-repair damage stage without allowing them to fail fully, while beams B211d and B221d were subjected to the maximum load at the pre-repair damage stage and were subjected to full failure.

Beams B211d and B221d were repaired using two CFRP sheets with widths of 100 mm and placed inclined at 45° on both sides of the RC beam between the applied load and the supports. In addition, beams B212d and B222d were repaired using three CFRP sheets (two with 100 mm width and one with 50 mm width) and placed vertically on both sides of the RC beam between the applied load and the supports.

The comparison is based on the ultimate repair capacity and the maximum CFRP sheet strain at failure for both the ACI and experimental results, and the results are shown in Table 8. The results showed variations in the difference between ACI Code and experimental results in terms of the ultimate shear capacity. For beam B211d, the ACI Code results were higher by approximately

Table 8 Comparison of ACI Code and experimental results for repair shear beam at 1.5d

| Beam | Case | Ultimate load capacity (kN) | | | CFRP debonding strain (μst) | | |
|--------|--|-----------------------------|----------|--------|--|----------|--------|
| | | Experimental | ACI Code | Dif. % | Experimental | ACI Code | Dif. % |
| B211 d | With stirrups & Damaged at failure load | 143 | 179.2 | 25.3 | 1,000 | 1,570 | 57 |
| B212 d | With stirrups & Damaged at maximum load | 165 | 171.6 | 4 | 500 | 1,490 | 198 |
| B221 d | Without stirrups & Damaged at failure load | 150 | 162.5 | 8.3 | 1,750 | 1,750 | 0 |
| B222 d | Without stirrups & Damaged at maximum load | 165 | 157.8 | -4.4 | 500 | 1,690 | 238 |

Table 9 Comparison of ACI Code and experimental results for repair shear beam at 1.5d

| Beam | Case | Ultimate load capacity (kN) | | |
|--------|--|-----------------------------|-------------------|--------|
| | | Experimental | Modified ACI Code | Dif. % |
| B211 d | With stirrups & Damaged at failure load | 143 | 143 | 0 |
| B212 d | With stirrups & Damaged at maximum load | 165 | 153 | -7.3 |
| B221 d | Without stirrups & Damaged at failure load | 150 | 154.8 | -3.2 |
| B222 d | Without stirrups & Damaged at maximum load | 165 | 165 | 0 |

25%, and for beam B222d, the ACI Code results were smaller by 4.4%. The difference in the CFRP strain is higher than the ultimate shear capacity, and the ACI values are higher than the experimental results, which indicates a smaller contribution from the CFRP sheets to the ultimate capacity. For the repaired beams with vertical CFRP sheets, the ACI Code results showed much higher values than the experimental results in terms of the CFRP strain, which indicates a smaller contribution from the CFRP sheets. The significant difference between the ACI and the experimental can be due to the assumption of the ACI while calculating the contribution of the concert, steel and CFRP to the ultimate capacity.

The same considerations that were considered when modifying the ACI Code equations for the shear capacity at quarter-span were considered. A reduction factor (RF_c) was applied to the contribution of the concrete, which was based on the pre-repair damage level. The CF_m value of 1.0 was used. The contribution factor for the CFRP sheets to the ultimate repaired shear capacity (CF^f) was applied to the V_f part in Eq. (15) of the ultimate repair capacity, and its value was adjusted based on the experimental results.

The results of the comparison of the ultimate shear capacity between the modified ACI equations and the experimental results are shown in Table 9. The modified ACI Code equations had a stronger agreement with the experimental results for all the beams, and the ACI Code results were smaller than the experimental. The reduction factor RF_c for the concrete contribution was 0.0, where the concrete is presumed to lose all its stiffness at the pre-repair damage stage. The contribution factor for the CFRP CF_f was 0.18 for the case of full failure at the pre-repair damage stage, which was B211d and B221d, where the shear cracks and deformation influence the bond between the externally bonded CFRP sheets and the concrete surface. For the cases where full failure was not allowed, which was beams B212d and B222d, the CF_f values were 0.3 with the shear crack defects being smaller.

4. Conclusions

From this study, the following conclusions can be drawn:

- The ACI Code model for calculating the ultimate flexural capacity of the CFRP repaired beams had smaller values than the experimental results because the ACI assumptions neglected the steel bars at the compression zone.
- The ACI Code model for calculating the ultimate shear capacity of the CFRP repaired beams had significantly higher results than the experimental results because the ACI question did not consider the pre-repair damage effect.
- The ACI Code models correlated better in the flexural capacity than the shear capacity. However, the differences between the ACI Code and experimental results are still significant.
- The modified models for predicting the flexural capacity by considering the effect of the steel reinforcement at the compression zone resulted in a better agreement with the experimental results.
- The modified model for predicting the shear capacity considered the following, and the results had a much better agreement with the experimental results:
 - i. Increased concrete contribution by considering the incline surface area,
 - ii. Decreased shear stirrups contribution by only considering the perpendicular component of its action,
 - iii. Add the contribution of the flexural reinforcement through the shear zone with an applicable contribution factor,
 - iv. Apply the concrete reduction factor to account for the loss of concrete stiffness due to the pre-repair damage level,
 - v. Apply the contribution factor for the contribution of the externally bonded CFRP sheet.

Acknowledgments

The author would like to acknowledge the financial assistance provided by University of Malaya. The author would also like to thank all the people who have contributed in any way to making this research possible.

References

- ACI 318 (2008), *Building Code Requirements for Structural Concrete*, American Concrete Institute, Farmington Hills, MI, U.S.A.
- ACI-440.2R (2008), *Guide for the Design and Construction of Externally Bonded FRP Systems For Strengthening Concrete Structures*, American Concrete Institute, Farmington Hills, MI, U.S.A.
- ACI-440.3R (2004), *Guide for Test Methods for Fiber Reinforced Polymers (FRP) for Reinforcing and Strengthening Concrete Structures*, American Concrete Institute, Farmington Hills, MI, U.S.A.
- ACI-440-2R (2000), *Design Guidance for Strengthening Concrete Structures Using Fiber Composite Materials*, American Concrete Institute, Farmington Hills, MI, U.S.A.
- ACI-440-2R (2002), *Guide for the Design and Construction of Externally Bonded FRP Systems for Strengthening Concrete Structures*, American Concrete Institute, Farmington Hills, MI, U.S.A.
- ACI-440R (1996), *State-of-the-Art Report on FRP for Concrete Structures, Manual of Concrete Practice*, American Concrete Institute, Farmington Hills, MI, U.S.A.

- ACI-440R (2007), *Report on Fiber-Reinforced Polymer (FRP) Reinforcement for Concrete Structures*, American Concrete Institute, Farmington Hills, MI, U.S.A.
- Ahmed A, A., Naganathan, S., Nasharuddin, K. and Fayyadh, M.M. (2015), "Repair effectiveness of CFRP and steel plates in RC beams with web opening: effect of plate thickness", *Int. J. Civil Eng.*, **13**(2), 234-244. <http://dx.doi.org/10.22068/IJCE.13.2.234>.
- Ahmed A, A., Naganathan, S., Nasharuddin, K., Fayyadh, M.M. and Jamali, S. (2016), "Repair effectiveness of damaged RC beams with web opening using CFRP and steel plates", *Jordan J. Civil Eng.*, **10**(2). <https://jjce.just.edu.jo/issues/paper.php?p=3534.pdf>.
- Alhawamdah, M. and Alqam, M. (2020), "Behaviour assessment of reinforced concrete columns externally rehabilitated with carbon fiber-reinforced polymers (CFRPs) subjected to eccentric loadings", *Jordan J. Civil Eng.*, **14**(1). 1-13.
- Al-Khafaji, A. and Salim, H. (2020), "Flexural strengthening of RC continuous T-Beams using CFRP", *Fibers*, **8**(6), 41. <https://doi.org/10.3390/fib8060041>.
- AL-Kharkhi, H. and Aziz, A. (2018), "Shear strengthening of reinforced self-compacted concrete hammer head beams using warped CFRP strips: Experimental and theoretical study", *Jordan J. Civil Eng.*, **12**(4), 629-636.
- Al-Sulaimani, G.J., Sharif, A., Basunbul, I.A., Baluch, M.H. and Ghaleb, B.N. (1994), "Shear repair for reinforced concrete by fiberglass plate bonding", *ACI Struct. J.*, **91**, 458-464.
- Anil, Ö. (2006), "Improving shear capacity of RC T-Beams using CFRP composites subjected to cyclic load", *Cement Concrete Compos.*, **28**(7), 638-649. <https://doi.org/10.1016/j.cemconcomp.2006.04.004>.
- Bakis, C.E., Bank, L.C., Cosenza, E., Davalos, J.F., Lesko, J.J., Machida, A., Rizkalla, S.H. and Triantafillou, T. (2002), "Fiber-reinforced polymer composites for construction - state of the art review", *J. Compos. Construct.*, **6**(2), 73-87. [https://doi.org/10.1061/\(ASCE\)1090-0268\(2002\)6:2\(73\)](https://doi.org/10.1061/(ASCE)1090-0268(2002)6:2(73)).
- Capozucca, R. and Cerri, M.N. (2002), "Static and dynamic behaviour of RC beam model strengthened by CFRP-sheets", *Construct. Build. Mater.*, **16**(2) 91-99. [https://doi.org/10.1016/S0950-0618\(01\)00036-8](https://doi.org/10.1016/S0950-0618(01)00036-8).
- Chaallal, O., Nollet, M.J. and Perraton, D. (1998), "Strengthening of reinforced concrete beams with externally bonded fiber-reinforced-plastic plates: Design guidelines for shear and flexure", *Canadian J. Civil Eng.*, **25**(4), 692-704. <https://doi.org/10.1139/l98-008>.
- Chen, J.F. and Teng, J.G. (2001), "Anchorage strength models for FRP and steel plates bonded to concrete", *J. Struct. Eng.*, **127**(7), 784-791. [https://doi.org/10.1061/\(ASCE\)0733-9445\(2001\)127:7\(784\)](https://doi.org/10.1061/(ASCE)0733-9445(2001)127:7(784)).
- Chen, J.F. and Teng, J.G. (2003), "Shear capacity of FRP-Strengthened RC Beams: FRP debonding", *Construct. Build. Mater.*, **17**(1), 27-41. [https://doi.org/10.1016/S0950-0618\(02\)00091-0](https://doi.org/10.1016/S0950-0618(02)00091-0).
- Colotti, V. and Spadea, G. (2001), "Shear strength of RC beams strengthened with bonded steel or FRP plates", *J. Struct. Eng.*, **127**(4), 367-373. [https://doi.org/10.1061/\(ASCE\)0733-9445\(2001\)127:4\(367\)](https://doi.org/10.1061/(ASCE)0733-9445(2001)127:4(367)).
- Dias, S.J.E. and Barros, J.A.O. (2010), "Performance of reinforced concrete T beams strengthened in shear with NSM CFRP laminates", *Eng. Struct.*, **32**(2), 373-384. <https://doi.org/10.1016/j.engstruct.2009.10.001>.
- El-Ghandour, A.A. (2011), "Experimental and analytical investigation of CFRP flexural and shear strengthening efficiencies of RC beams", *Construct. Build. Mater.*, **25**(3), 1419-1429. <https://doi.org/10.1016/j.conbuildmat.2010.09.001>.
- El-Mihilmy, M. and Tedesco, J.W. (2000), "Analysis of reinforced concrete beams strengthened with FRP laminates", *J. Struct. Eng.*, **126**(6), 684-691. [https://doi.org/10.1061/\(ASCE\)0733-9445\(2000\)126:6\(684\)](https://doi.org/10.1061/(ASCE)0733-9445(2000)126:6(684)).
- El-Taly, B., HasabElnaby, Y. and Meleika, N. (2018), "Structural performance of precast–prestressed hollow core slabs subjected to negative bending moments", *Asian J. Civil Eng.*, **19**, 725-740. <https://doi.org/10.1007/s42107-018-0061-0>.
- Fayyadh, M.M. and Razak, H.R. (2012), "Assessment of adhesive setting time in reinforced concrete beams strengthened with carbon fibre reinforced polymer laminates", *Mater. Des.*, **37**, 64-72. <https://doi.org/10.1016/j.matdes.2011.12.031>.
- Fayyadh, M.M. and Razak, H.R. (2012), "Assessment of effectiveness of CFRP repaired RC beams under different damage levels based on flexural stiffness", *Construct. Build. Mater.*, **37**, 125-134. <https://doi.org/10.1016/j.conbuildmat.2012.07.021>.
- Fayyadh, M.M. and Razak, H.R. (2014), "Analytical and experimental study on repair effectiveness of

Modified models to predict the ultimate flexural and shear capacities of CFRP repaired RC beams

- CFRP sheets for RC beams”, *J. Civil Eng. Managem.*, **20**(1), 21-31. <https://doi.org/10.3846/13923730.2013.799095>.
- Khalifa, A. and Nanni, A. (2000), “Improving shear capacity of existing RC T-section beams using CFRP composites”, *Cement Concrete Compos.*, **22**(3), 165-174. [https://doi.org/10.1016/S0958-9465\(99\)00051-7](https://doi.org/10.1016/S0958-9465(99)00051-7).
- Khalifa, A., Gold, J.W., Nanni, A. and Abdel-Aziz, M.I. (1998), “Contribution of externally bonded FRP to shear capacity of RC flexural members”, *J. Compos. Construct.*, **2**(4), 195-203. [https://doi.org/10.1061/\(ASCE\)1090-0268\(1998\)2:4\(195\)](https://doi.org/10.1061/(ASCE)1090-0268(1998)2:4(195)).
- Lam, L. and Teng, J.G. (2001), “Strength of RC cantilever slabs bonded with GFRP strips”, *J. Compos. Construct.*, **5**(4), 221-227. [https://doi.org/10.1061/\(ASCE\)1090-0268\(2001\)5:4\(221\)](https://doi.org/10.1061/(ASCE)1090-0268(2001)5:4(221)).
- Lee, H.K., Cheong, S.H., Ha, S.K. and Lee, C.G. (2011), “Behavior and performance of RC T-Section deep beams externally strengthened in shear with CFRP sheets”, *Compos. Struct.*, **93**(2), 911-922. <https://doi.org/10.1016/j.compstruct.2010.07.002>.
- Li, A., Assih, J. and Delmas, Y. (2001), “Shear strengthening of RC beams with externally bonded CRRP sheets”, *J. Struct. Eng.*, **127**(4), 374-380. [https://doi.org/10.1061/\(ASCE\)0733-9445\(2001\)127:4\(374\)](https://doi.org/10.1061/(ASCE)0733-9445(2001)127:4(374)).
- Malek, A.M. and Patel, K. (2002), “Flexural strengthening of reinforced concrete flanged beams with composite laminates”, *J. Compos. Construct.*, **6**(2), 97-103. [https://doi.org/10.1061/\(ASCE\)1090-0268\(2002\)6:2\(97\)](https://doi.org/10.1061/(ASCE)1090-0268(2002)6:2(97)).
- Malek, A.M. and Saadatmanesh, H. (1998), “Ultimate shear capacity of reinforced concrete beams strengthened with web-bonded fiber reinforced plastic plates”, *ACI Struct. J.*, **95**(4), 391-399.
- Meier, U. (1992), “Carbon fiber reinforced polymers: Modern materials in bridge engineering”, *Struct. Eng. Int.*, **2**(1), 7-12. <https://doi.org/10.2749/101686692780617020>.
- Mohamed-Ali, M.S., Oehlers, D.J. and Seracino, R. (2006), “Vertical shear interaction model between external FRP transverse plates and internal steel stirrups”, *Eng. Struct.*, **28**(3), 381-389. <https://doi.org/10.1016/j.engstruct.2005.08.010>.
- Pellegrino, C. and Modena, C. (2002), “Fiber-reinforced polymer shear strengthening of reinforced concrete beams with transverse steel reinforcement”, *J. Compos. Construct.*, **6**(2), 104-111. [https://doi.org/10.1061/\(ASCE\)1090-0268\(2002\)6:2\(104\)](https://doi.org/10.1061/(ASCE)1090-0268(2002)6:2(104)).
- Saadatmanesh, H. and Ehsani, M.R. (1991), “RC Beams strengthened with GFRP plates I: Experimental study”, *J. Struct. Eng.*, **117**(11), 3417-3433. [https://doi.org/10.1061/\(ASCE\)0733-9445\(1991\)117:11\(3417\)](https://doi.org/10.1061/(ASCE)0733-9445(1991)117:11(3417)).
- Saadatmanesh, H. and Malek, A.M. (1998), “Design guidelines for flexural strengthening of RC beams with FRP plates”, *J. Compos. Construct.*, **2**(4), 158-164. [https://doi.org/10.1061/\(ASCE\)1090-0268\(1998\)2:4\(158\)](https://doi.org/10.1061/(ASCE)1090-0268(1998)2:4(158)).
- Shaw, I.D. and Andrawes, B. (2017), “Finite element analysis of CFRP laminate repairs on damaged end regions of prestressed concrete bridge girders”, *Advan. Comput. Des.*, **2**(2), 147-168. <https://doi.org/10.12989/acd.2017.2.2.147>
- Stallings, J.M., Tedesco, J.W., El-Mihilmy, M. and McCauley, M. (2000), “Field performance of FRP bridge repairs”, *J. Bridge Eng.*, **5**(2), 107-113. [https://doi.org/10.1061/\(ASCE\)1084-0702\(2000\)5:2\(107\)](https://doi.org/10.1061/(ASCE)1084-0702(2000)5:2(107)).
- Teng, J.G., Chen, J.F., Smith, S.T. and Lam, L. (2001), *FRP-Strengthened RC Structures*, John Wiley & Sons England, U.K.
- Triantafyllou, T.C. and Plevris, N. (1992), “Strengthening of RC Beams with epoxy-bonded fiber-composite materials”, *Mater. Struct.*, **25**, 201-211. <https://doi.org/10.1007/BF02473064>.
- Vuković, N.K., Jevrić, M. and Zejak, R. (2020), “Experimental analysis of RC elements strengthened with CFRP strip”, *Mech. Compos. Mater.*, **56**, 75-84. <https://doi.org/10.1007/s11029-020-09861-x>.
- Xie H.B. and Wang Y.F. (2019), “Reliability analysis of CFRP-strengthened RC bridges considering size effect of CFRP”, *Materials*, **12**(14), 2247. <https://doi.org/10.3390/ma12142247>.